



## Implementation Optimal Location of SSSC to Improve the Efficiency on IEEE New England Transport Network (100 kV)

Najib Ababssi<sup>1\*</sup>      Azeddine Loulijat<sup>1</sup>      El alami Semma<sup>1</sup>

<sup>1</sup>Laboratory of Engineering Industrial Management and Innovation,  
 Faculty of Science and Technique, Hassan I University, Settat, Morocco

\* Corresponding author's Email: nababssi@gmail.com

---

**Abstract:** In electrical power systems, the major safety constraints in a high voltage power system are the stability limit and the voltage profile. This paper aims to improve the voltage stability of the IEEE-39 bus New England transmission system, where we used a flexible AC transmission system (FACTS), in particular a STATIC synchronous serie COMPensator (SSSC) controller. The method proposed in this paper is based on the continuation power flow (CPF) technique coupled with bifurcation theory, to select the optimal location of the FACT device. The effectiveness of the proposed method is verified by means of a simulation test using the software power system analysis toolbox [PSAT]. The results obtained show that the SSSC has a better local behaviour (i.e. in the area where it is implemented). To be effective, an SSSC must be placed on a line with maximum powers at the point of collapse. The simulation results demonstrate the effectiveness of the proposed SSSC scheme in improving the stability of the IEEE (100KV) power system.

**Keywords:** Flexible alternatif current transmission system (FACTS), Continuous power flow (CPF), STATic synchronous serie COMPensator (SSSC), Power system analysis toolbox (PSAT) software, Theory of bifurcation, Voltage stability systems, Load factor ( $\lambda$ ).

---

### 1. Introduction

As time passes, the demand on the electricity grid increases in an attempt to meet the need for energy supply [1]. Electrical systems operating close to their thermal limits, either due to increased load or severe contingencies, will lead to a situation where the system will no longer remain in the safe operating area [2]. In the modern electricity system, the improvement of power quality and the provision of a certain amount of power at the lowest cost is considered a major issue [3]. One of the concerns of planners and operators of electricity networks is to ensure that the voltages on the various busbars of the network remain, despite everything, within prescribed limits, especially under heavy load conditions and/or following plausible incidents. The mechanism behind voltage collapse is voltage instability and the resulting catastrophe is voltage collapse. Hence, detection of this potential collapse

in power systems is essential to maintain voltage stability under high demand conditions.

Maintaining the voltage stability in a power system is one of the main problems in the power system operation due to the huge demand for which there is a need to add the installation [4]. Extensive studies have been carried out and suggest various ways to improve the voltage stability of the network, to maintain code compliance and to compensate for reactive power in the system [1]. The study of the electrical system and in particular the voltage stability in the presence of flexible AC transmission systems (FACTS) devices is an interesting topic that has received much attention in the literature [5]. FACTS controllers are the most reliable option, regardless of the upgrade of the electrical networks [6]. These FACTS controllers provide a range of interesting capabilities such as power flow control, reactive power compensation, voltage regulation, improved transient stability and, potentially, a lower

cost than most alternative transmission system enhancement techniques [7, 8]. To increase the gain of the system stability margin, FACTS devices provide an appropriate control strategy [9]. The control of active and reactive power flow and bus voltage levels is one of the vital factors in the reliable and efficient development of the power system [10]. This paper uses a FACT controller: the static synchronous series compensator (SSSC), one of the main FACTS devices, consisting of a voltage converter and a transformer connected in series with the transmission line, to select an optimal location, to study the system responses during voltage collapse, to minimise total losses and to increase system reliability in order to improve the stability of the power system [2, 11-13]. The commercial version of the power system analysis toolbox [PSAT], [14] was used for the voltage stability analysis of the standard New England 39 bus (100 KV) transmission system [15].

Several methods for studying and analysing voltage stability have been presented by different researchers. The main approaches recently used are: particle swarm optimisation (PSO), Newton-Raphson (NR), genetic algorithm (GA) and metaheuristics.

The disadvantages of these methods can be summarised as follows: (PSO) is the high number of setting parameters and the use of archives, (NR) is its high cost and the singularity of the Jacobian matrix at the collapse point, (GA) is its cost in computation time, since it handles several solutions simultaneously. The fitting of a GA is delicate [15], the metaheuristic method is often less powerful than exact methods on certain types of optimisation problems. Nor do they guarantee the discovery of the global optimum in a finite time.

In [16] the authors studied the stability of the power system using CPF. In [17] the authors used CPF to simulate the quasi-stable state of an electrical system. In [18], the simulation of dynamic load restoration was developed using CPF. The CPF was used in [19] for the study of voltage stability as a function of load evolution at the boundary between the transmission and distribution networks of electric power. With the CPF the solution to a bifurcation point of the variation of the voltage  $V$  versus the reactive power  $Q$  consumed was found by plotting the  $Q$ - $V$  curves was used in [20]. In [21] the authors proposed a stability improvement using a FACTS device based on static VAR compensator VSC. The active power flow and voltage profile are improved by changing the reactance using the SSSC. The disadvantage of this method is the control of the controller voltage  $V_{dc}$ . Despite the undeniable

advantages of the CPF, it does have its drawbacks. It suffers from a slow convergence speed, which makes it unfavourable for the analysis of the static voltage stability of large power systems.

In contrast to these methods, the (CPF) method coupled with the bifurcation theory does not have these shortcomings mentioned above. The CPF ensures greater precision in the assessment of the stability margin. The CPF finds the solutions of the reformulated power flow equations to determine the voltage profile as a function of the load increment up to the point of collapse. Bifurcation theory is the most accepted analytical tool for studying the phenomena of stress collapse, it can also study the behaviour of the system in the vicinity of collapse or unstable points. These advantages make the CPF method and the bifurcation theory more suitable for voltage stability analysis. Thus we chose the (CPF) method coupled with the bifurcation theory. The IEEE 39 bus test network is used to verify the performance of the proposed method.

In this paper, we propose a new method to calculate the maximum load point, in order to place the SSC, based on the CPF and the bifurcation theory. In order to select the optimal location of the SSSC, a parameterised equation based on the active and reactive power equations at the collapse point was added to the NR method. Therefore, the bus that represents a maximum increase in active and reactive power at the point of collapse is the weakest bus in the system. The application of this new method coupled with the bifurcation theory to the IEEE 39 bus test network shows that the maximum load point can be obtained accurately. The proposed method is effective, precise and gives very interesting results to those obtained by the CPF.

The rest of the paper is structured as follows: formulation of the research method, the objective functions for the study of the stability of the test network is explained in section 2, the proposed method for studying stability : Modelling of the FACTS "SSSC" device coupled to the network, la détection des bus les plus faibles du système, location and impact of SSSC and voltage level in section 3, the simulation tests and discussion are provided in section 4 followed by the conclusions in section 5.

## 2. Research method

In this section, the objective function of this paper is to find the optimal location of the SSSC device to improve the stability of the power system. This paper investigates the combination of three objective functions: maximising the load margin,

improving the system voltage profile and minimising active and reactive power losses. In this paper, the local performance of the electrical system is improved by using the serial FACTS device which is SSSC.

## 2.1 Load margin index ( $\lambda$ ) and power flow

In general, the CPF method starts with the baseline conditions using conventional Load Flow (LF) solutions from the Newton-Raphson algorithm to calculate the load factor  $\lambda$ . The (LF) equation is written in matrix form, or the Jacobian matrix  $J$ . The conventional load flow equation is defined by relationship (1):

$$g(x) = \begin{bmatrix} P(\theta, V) - P_i \\ Q(\theta, V) - Q_i \end{bmatrix} = 0 \quad (1)$$

where,  $P(\theta, V)$  and  $Q(\theta, V)$  are respectively the vectors of the active and reactive powers of the network,  $P_i$  and  $Q_i$  are respectively the vectors of the active and reactive power injected from each bus of the network.

To find out the state of the power system for different load factors, a state variable  $\lambda$  is added to the Load Flow LF equation. This is done by reformulating the Load Flow equation to introduce a load parameter  $\lambda$ , so one can obtain the plot of  $V$  by varying  $\lambda$ .

For the study of voltage collapse phenomena an analytical tool called the bifurcation theory is used. It is a tool that is able to classify instabilities, to study the behaviour of the system in the vicinity of collapse or unstable points.

In bifurcation theory, the system equations depend on a set of parameters with state variables. The equation system of the multiquadric polyharmonic equation PMQ, after reformulation, then becomes that of Eq. (2): [15].

$$f(x, \lambda) = 0 \quad (2)$$

Where  $f$  is the power flow equation,  $x$  is the dependent variables ( $x = (V, \theta)$ ) or solution of the equation  $f$  and  $\lambda$  is the load factor.

The stability / instability properties are assessed by 'slowly' varying a parameter used to study the proximity of the system to voltage collapse called load factor  $\lambda$ , which changes the powers of the generator and the load, hence Eq. (3):

$$\begin{cases} P_{G1} = (1 + \lambda)(P_{G0} + P_S) \\ P_{L1} = (1 + \lambda)(P_{L0} + P_D) \end{cases} \quad (3)$$

Where  $P_{G0}$  is the active power of the generator,  $P_{L0}$  is the active power of the load,  $P_S$  is the supply bids and  $P_D$  is the demand bids.

Consider the power flow equations defined in relation (3), where the load factor  $\lambda$  affects only the power variables  $P_S$  and  $P_D$ .

The powers that multiply  $\lambda$  are called the steering powers. Eq. (3) differ from the model generally used in the continuous power flow (CPF) analysis, which gives Eq. (4):

$$\begin{cases} P_{G2} = (P_{G0} + \lambda P_S) \\ P_{L2} = (P_{L0} + \lambda P_D) \end{cases} \quad (4)$$

The indices 0, 1 and 2 denote the base case, the first point and the second point of power directions respectively. The active powers of the generator and the line depend on the supply bids and demand bids.

In the power flow calculations, the power  $P_{G0}$  is taken as constant and the voltage  $V_i$  can be kept at a constant set value in the module. The phase  $\theta_i$  and the reactive power depend on the state of the network. When  $Q_{G0}$  exceeds one of these limits, its value is set to this limit value and the voltage can no longer be controlled. The bus is no longer considered a generator but a load.

With  $P_{G0}$  active power delivered by the generator to bus  $i$ ,  $Q_{G0}$  reactive power delivered by the generator to bus  $i$ ,  $V_i$  complex voltage at bus  $i$ ,  $\theta_i$  : phase shift of the voltage at bus  $i$ .

The production limits of the generators are defined by:

$$\begin{aligned} P_{G0min} &\leq P_{G0} \leq P_{G0max} \\ Q_{G0min} &\leq Q_{G0} \leq Q_{G0max} \end{aligned}$$

In typical bifurcation diagrams, voltages are plotted as a function of  $\lambda$ , resulting in  $V(p)$  curves that determine the voltage collapse points where the value of  $\lambda$  is maximum.

## 2.2 Power loss index (PLI)

The objective of reducing active and reactive power losses is achieved by choosing the best combination of variables, which minimises the total power losses of the power system. Based on this objective function, the active and reactive power losses are calculated with and without FACTS controller. The method proposed in this document is based on the CPF technique. Using the CPF, the active and reactive power losses are calculated. The behaviour of the test system considered with and without FACT, for lines 15, 45 and 48 respectively and different loading conditions is studied. The PLI

at the stability margin is studied for the three cases independently.

### 2.3 Voltage level

The amplitude of the bus voltage must be kept within the permissible range to ensure a good service. The voltage profile (voltage level) at the network bus allows the variation of the voltage at each network node to be assessed in order to control the stability of the network within its limits, to ensure that generation and consumption are matched. In this section, the objective function takes into account the voltage levels. In fact, power system operators impose a tolerance of  $\pm 5\%$  on the voltage of the transmission network to guarantee the quality of electricity distribution. We will therefore take  $U_{min}=0.95p.u$  and  $U_{max} = 1.05 p.u$  (i.e. 95 KV and 105 KV respectively for our nominal 100 KV transmission network). It is obvious that the SSSC, installed at the weakest node in the system, should provide a better voltage profile at the point of voltage collapse compared to the baseline state. In this paper, the CPF technique is used to obtain the voltage profile of the IEEE-39 bus transmission network, without and with SSSC, when varying the active power demand of a PQ bus.

### 3. Continuous power flow calculation

Serval simulation tools have been used in the analysis and study of electrical networks such as (Matlab, EMTP, Etap, PowerWorld, PSAT,... etc). In this paper, the PSAT [14] software is used for the analyse of the voltage stability of a transmission system, by performing two static functions: (Power Flow- PF) and (Continuous Power Flow- CPF). In this section, we focus on the CPF continuous power flow method. With the CPF one can find the bifurcation point of the system by systematically increasing the load factor  $\lambda$  of the system. The CPF technique is a very effective tool for calculating the trajectory of one or more parameters of the system under study. It also makes it easy to study the voltage stability of electrical systems. In this study, the CPF is used to plot the voltage profile (V magnitude) and the total HV power system loss profile as a function of the active and reactive power variation of a system network bus.

Before applying the CPF method to study the voltage stability of the transmission network, it is essential to model the FACT device that is involved in this analysis. Fig. 2 shows the equivalent model of the SSSC coupled to the grid to find the solutions of a series of successive power flows and determine

the voltage profile as a function of the load evolution up to the point of collapse. Voltage instability phenomena can range in time from seconds to hours and have been studied using a variety of static and dynamic models, including regulators and power electronic devices. In this document the FACT device used is the SSSC. The SSSC has been selected to be placed in a suitable location and of adequate size to improve the performance of the IEEE (100 kV) power grid.

### 3.1 Modelling of SSSC

In order to study the impact of FACTS on the voltage improvement of power systems, appropriate models need to be developed. We would like to mention that several software packages incorporate these models. In this paper we will present the mathematical model of the SSSC shown in Fig. 2.

This FACTS device has been selected to be placed in a suitable location and of adequate size to improve the performance of the IEEE (100 kV) power grid.

The series synchronous static compensator (SSSC) is probably the most widely used FACTS device in today's power systems [3]. The SSSC is connected in series with the power transmission line, produces a controllable voltage and is used to improve the stability and performance of the power system [9], [10], [13]. Its circuit design includes a voltage source converter (VSC), a DC capacitor and a series coupling transformer. The coupling transformer is connected in series with the electrical system that couples the SSSC with the transmission line [13]. The SSSC voltage in series with the line at  $90^\circ$  lagging or leading to line current. If injected voltage lags line current, it realizes capacitive reactance in the line. Effective line reactance will be reduced, which results in increase in active power flow in the line. Similarly, if injected voltage leads line current at  $90^\circ$ , it realizes inductive reactance in the line which increases effective line reactance [22].

The SSSC can acquire an energy storage element for momentary active power compensation which results in efficient maintenance of power system stability. An SSSC is therefore modelled as a series voltage source, Fig. 3 shows an SSSC inserted in a two-machine network and its voltage vector diagram.

This operation is similar to series compensation by a capacitor. If we write the voltage generated by the SSSC as a function of the line current, we obtain the same result as in a series compensation with a capacitor. This voltage is given in Eq. (5):

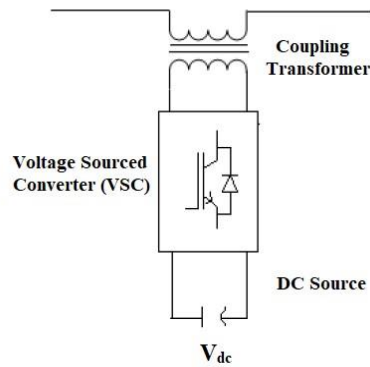


Figure. 1 Basic scheme of the SSSC [9]

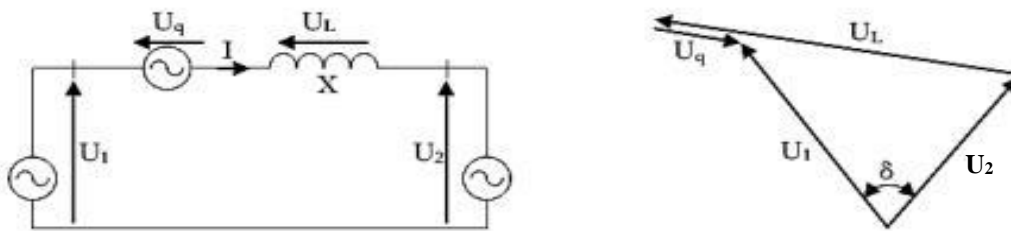


Figure. 2 Serial voltage source for compensation

$$\underline{U} = -jX_c I \tag{5}$$

Where  $X_c$  is the capacitive reactance of the capacitor.

But as the SSSC is a voltage source, it can then maintain a constant voltage as it controls independently of the line current. In this case, the SSSC can increase or decrease the power flow through the line simply by controlling the voltage injected in series with the line. As the SSSC is a reactive source, the generated voltage is perpendicular to the line current, this current is given in Eqs. (6), (7) and (8) :

$$I = \frac{U_1 - \underline{U}_q - U_2}{jX} \tag{6}$$

$$I = \frac{1}{jX} ((U_1 - U_2) - \underline{U}_q \cdot \frac{(U_1 - U_2)}{|U_1 - U_2|}) \tag{7}$$

$$I = \frac{j(U_1 - U_2)}{X} (1 - \frac{\underline{U}_q}{|U_1 - U_2|}) \tag{8}$$

This equation shows that, in the absence of the SSSC, the voltage drop across  $X$  is  $(U_1 - U_2)$ . If we take  $\underline{U}_2$  as the SSSC reference the SSSC, so Eq. (9):

$$\underline{U}_2 = U_2 \tag{9}$$

And (17):

$$\underline{U}_1 = U_1(\cos \delta + j \sin \delta) \tag{10}$$

If we consider that (18) :

$$|\underline{U}_1 - \underline{U}_2| = \sqrt{U_1^2 + U_2^2 - 2U_1U_2 \cos \delta} \tag{11}$$

This gives us power through the line, Eq. (12) :

$$P = \frac{U_1U_2 \sin \delta}{X} (1 - \frac{U_q}{\sqrt{U_1^2 + U_2^2 - 2U_1U_2 \cos \delta}}) \tag{12}$$

Therefore, the transmitted power  $P$  is a function of the injected voltage. The transmitted power as a function of the angle  $\delta$ .

#### 4. Results and discussion

The performance of the proposed method is evaluated by simulation on IEEE lines 15, 45 and 48, which are part of the 100 kV New England transmission system. The one-line diagram of the test system is shown in Fig. 3 [15]. This network operates at 100 kV and has 10 generators ( $P_{Gtotal} = 6.19$  Gw,  $Q_{Gtotal} = 1.13$  Gvar) and 39 buses, of which 19 are load buses and 48 routes. The software [PSAT] [14]. is used for the implementation of SSSCs on the suitable line to improve the efficiency of the transport network.

##### 4.1 Detection of the weakest bus in the system

In order to study the voltage collapse point, it is

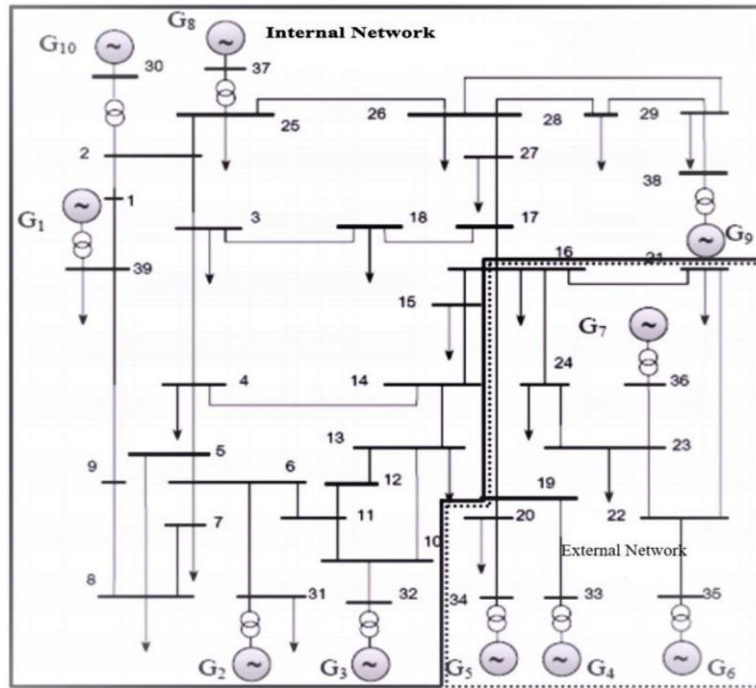


Figure. 3 The IEEE 39-Bus test network

Table 1. Weakest bus ranking in the 3areas

Area 1(Rank order )	Area 2 (Rank order )	Area 3 (Rank order )
8,7,5,6,4,12,14	3, 18, 17,27	15,16,24,21,28

Table 2. FP results for buses feeding critical lines in the test network

Bus [p.u.]	V [p.u]	phase[rad.]	P gen[p.u.]	Q gen[p.u.]	P load [p.u.]	Q load[p.u.]
BUS08	0.63731	-0.80455	0	0	11.9035	4.0135
BUS09	0.88016	-0.76257	0	0	0	0
BUS22	0.88171	-0.06877	0	0	0	0
BUS29	0.90865	-0.13955	0	0	6.4649	0.61342
BUS35	1.0492	0.17356	15.1459	15.7144	0	0
BUS38	1.0265	0.18789	19.3404	11.3176	0	0

Table 3. FP results for critical lines in the test network

From Bus	To Bus	Line	P Flow (p.u)	Q Flow (p.u)	P Loss (p.u)	Q Loss (p.u)
8	9	15	-0.91415	-4.2695	0.10425	1.4208
22	35	45	-15.1459	-9.5271	0	6.1873
29	38	48	-18.9592	-3.8828	0.38127	7.4347

necessary to first detect the weakest bus in the system. From Fig. 3, representing the IEEE 39-bus test network, Table 1 representing the ranking of the weakest buses in the system obtained by the PF method, Fig. 4(a) illustrating the voltage profile curve of the IEEE 39-bus network and Figs. 4(b), 4(c), and 4(d) illustrating the V(p) curves, of the three zones, obtained by the CPF method. The calculation of the CPF on the network without FACT, showed that the weakest bus in the system is bus 8 in zone 1, as it tends to the voltage collapse point before the other buses (Fig. 5(b)). Therefore, it is the most sensitive bus to the variation of voltage

versus reactive power. The maximum loading point occurs at  $\lambda = 2.2806$  p.u.

### 4.2 Location and impact of SSSC

The CPF method coupled with the bifurcation theory proposed in this paper, is executed on three lines of the system to determine the optimal placement of the FACTS SSSC device according to the optimisation constraints. The CPF method coupled with bifurcation theory is used to select the optimal location of the SSSC in order to improve the voltage profile and decrease the active and reactive losses of the transmission system. According to the



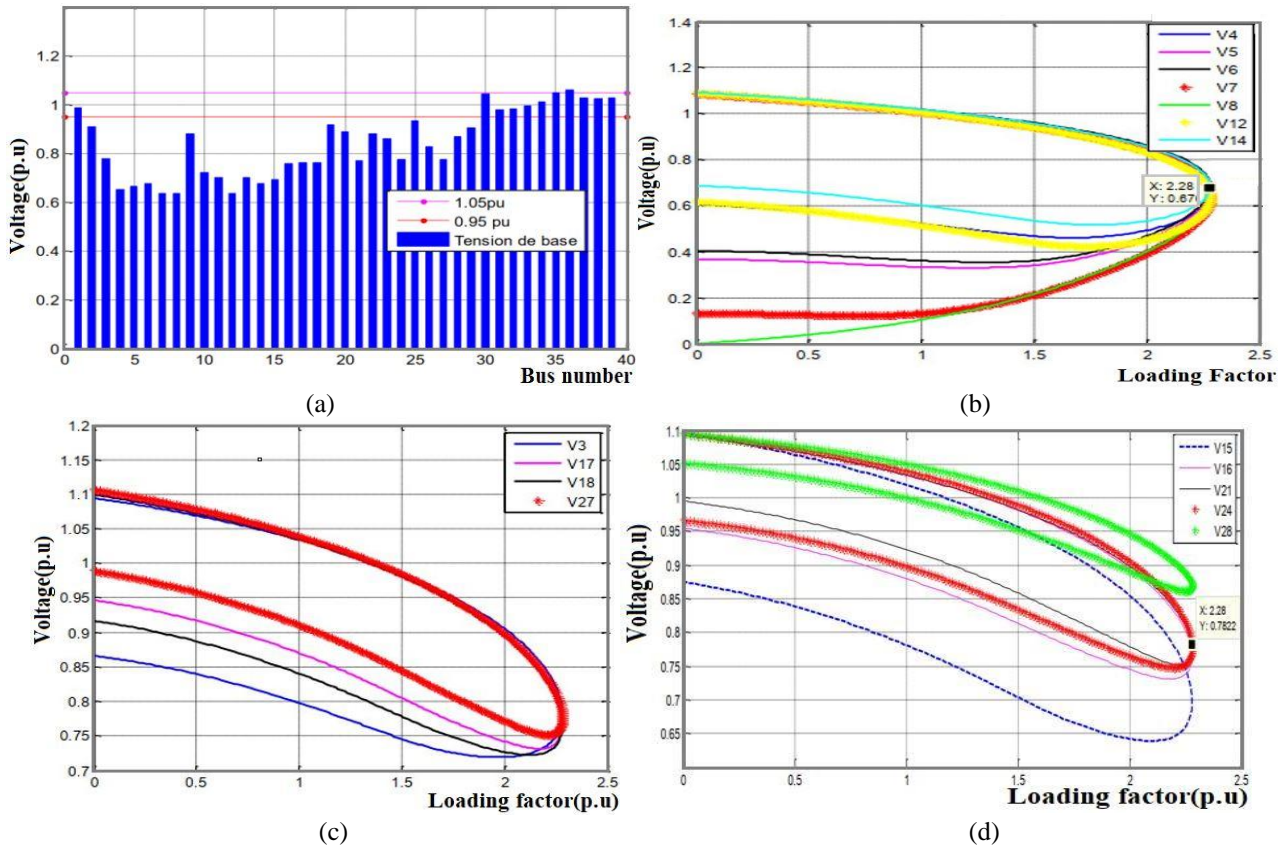


Figure. 4: (a) IEEE 39-bus network voltage profile and V(P) curves for (b) area 1 of the System (basic state), (c) area 2 of the System (basic state), and (d) area 3 of the System (basic state)

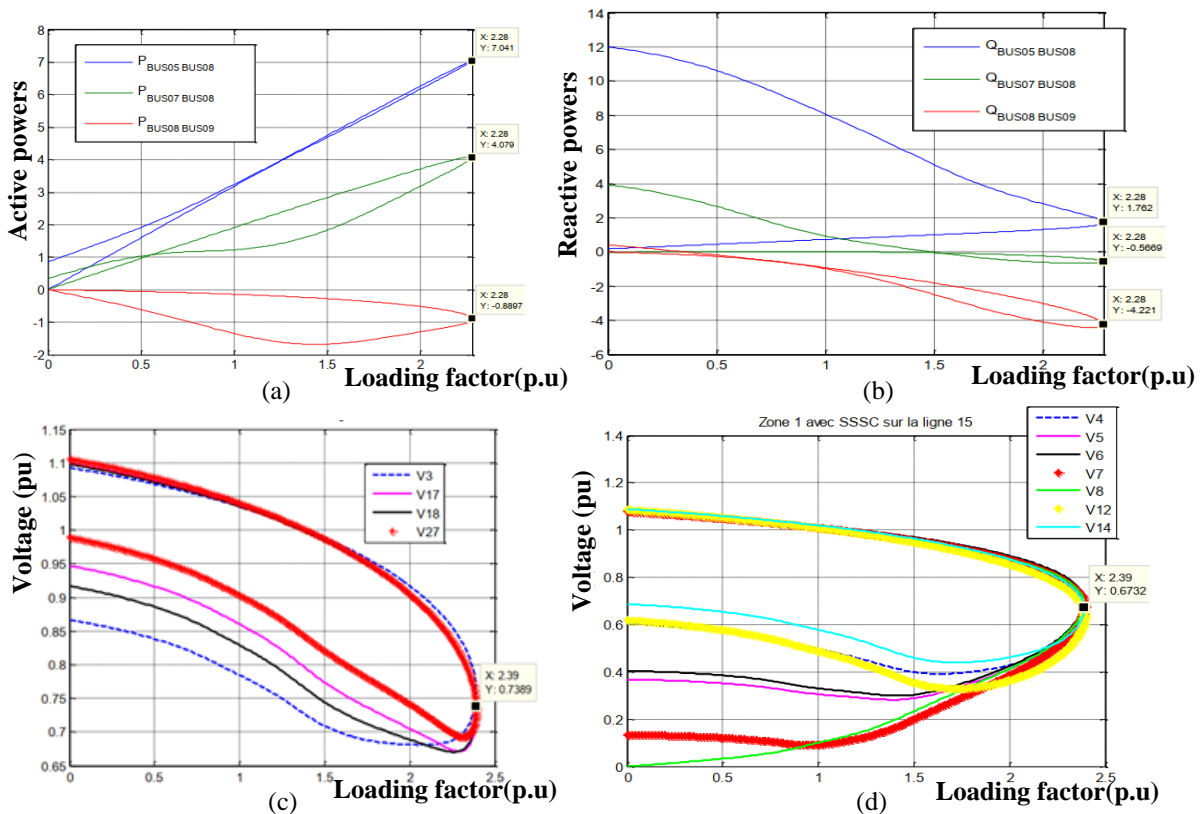


Figure. 5 Maximum powers at the point of collapse: (a) Reactive, (b) Active and V(P) curve of, (c) area 2 with SSSC on line 15, and (d) area 1 with SSSC on line 15

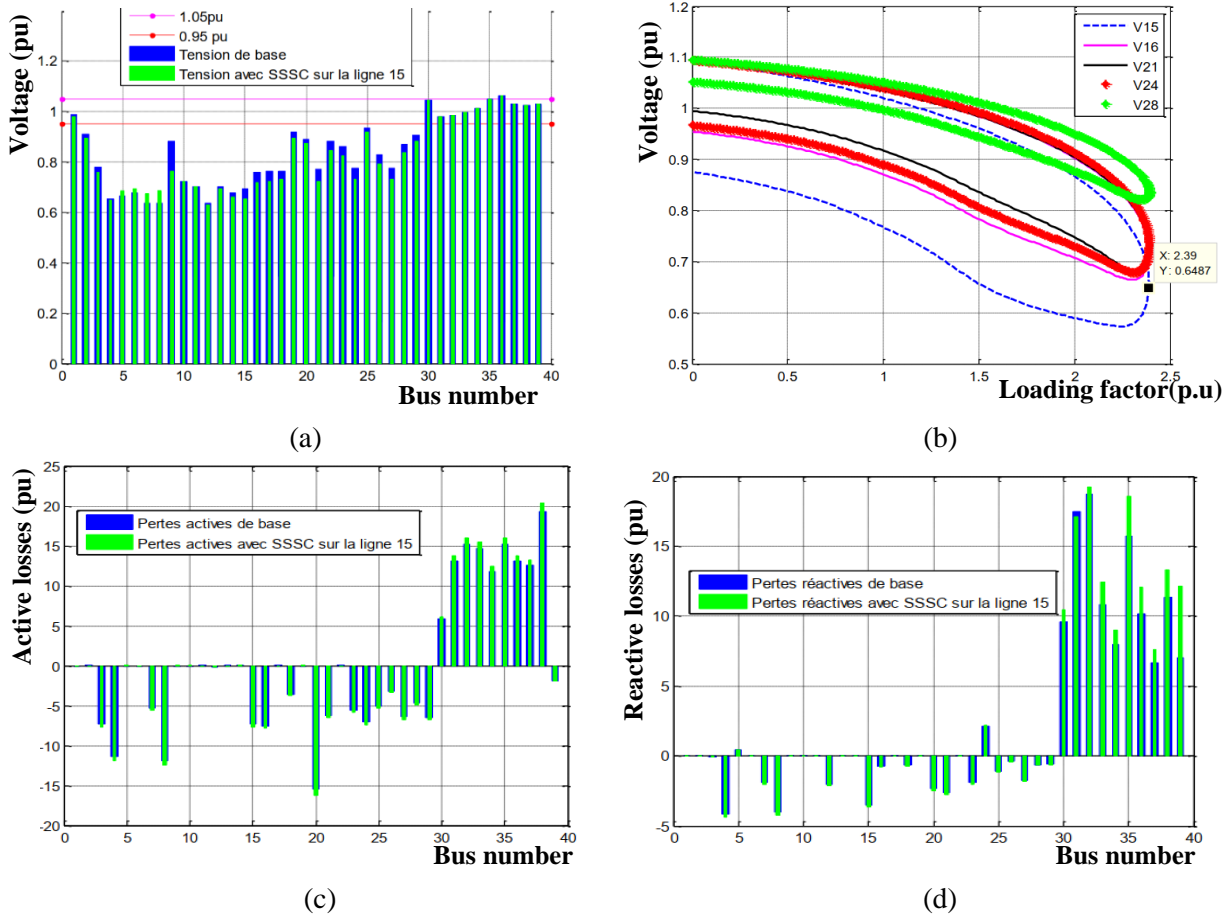


Figure. 6 : (a) System voltage profiles with SSSC on line 15, (b) V(P) curve of area 3 with SSSC on line 15 and power loss profiles with SSSC on line 15, (c) Active, and (d) Reactive

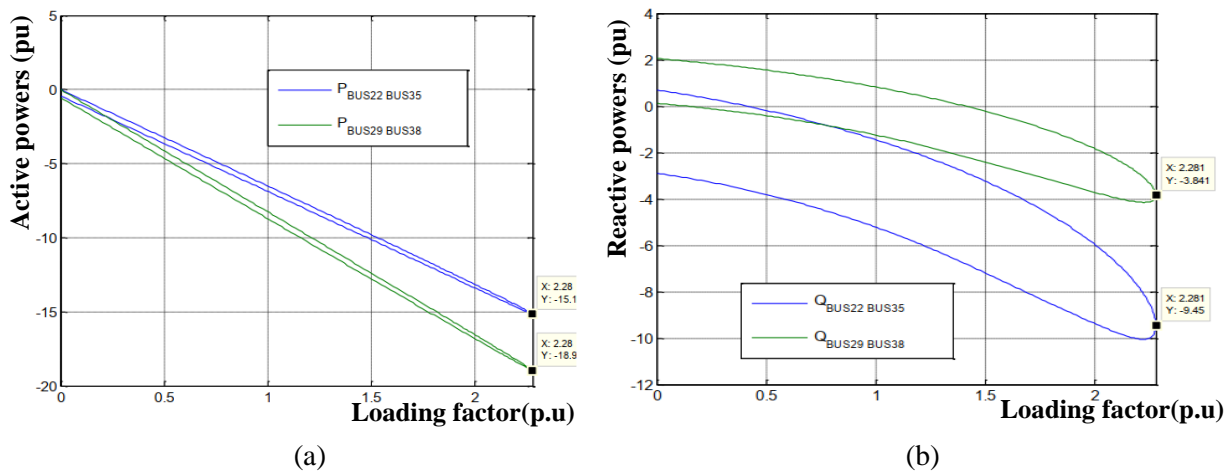


Figure. 7 Maximum powers at the collapse point of area 3: (a) Active and (b) Reactive

one-line diagram of the IEEE 39-bus electrical system shown in Fig. 3, bus 8 is normally supplied by three lines, 8-5, 8-7 and 8-9. The three lines are allocated slots for the installation of the SSSC controller. Therefore, lines 15, 45 and 48 are shown for the SSSC locations respectively. Similarly, the optimal location of the SSSC on one of these lines will be based on the maximum power increase at the point of voltage collapse.

Figs. 5(a) and 5(b) clearly show that the active and reactive powers on line 15 between buses 8 and 9 are maximum at the voltage collapse point. The simulation results, after insertion of the FACT SSSC device on line 15, are shown in Figs. 5(c), 5(d), and 6(b) which represent the V(P) curves of zones 1, 2 and 3 respectively, using the response of the CPF method. From these figures it can be seen that the bifurcation point occurs at a higher load value,  $\lambda =$



2.39 p.u (Fig. 6(b)).

From Figs. 6(a), 6(c), and 6(d) showing the voltage profile and the real and reactive loss profile curves respectively, it is evident that the SSSC inserted on line 15, bus 8-9 has not improved the voltage profile and the real and reactive loss profile at the voltage collapse point. The voltages of the buses (8-9) are lower than the desired value. Similarly, it is observed that the reactive losses on line 15 reach the maximum degree of 15.3 p.u.

Figs. 7(a) and 7(b) illustrate the behaviour of real and reactive power at the collapse point to determine the optimal value and location of the SSSC during the optimisation process. It can be seen from the simulations that there are two critical situations when the voltage collapses: on line 45 between buses 22 and 35 and on line 48 between buses 29 and 38. Furthermore, the overall performance is not improved for all buses in the system.

### 4.3 SSSC inserted on line 45

In order to improve both the voltage profile of

the system and to reduce the real and reactive losses after the addition of the SSSC device. We first place the SSSC controller on line 45 between buses 22 and 35. Figs. 8(a), 8(b), 8(c), and 8(d) show the V(P) curves, voltage profile and real and reactive losses respectively. The results show that the voltage profile is better for SSSC inserted on line 45 than for SSSC inserted on line 15, for a load demand of 2.34 p.u. From Fig. 8(b), it is evident that the voltage stability margin of line 45 is improved as the voltage collapse point becomes higher  $\lambda = 2.34$  p.u, compared to the baseline state  $\lambda = 2.28$  p.u.

Figs. 9(a), 9(b), 9(c), and 9(d) show the V(P) curves, the voltage profile and the real and reactive loss profile of the test system after the installation of the FACT SSSC devices, respectively. The simulation results show that the voltage profile, after the addition of the SSSC on line 48, is not better compared to the SSSC inserted on line 45. While the active and reactive loss profile after adding SSSC on line 48 is better than that of SSSC inserted on line 45. Therefore, the reduction rate of real and reactive power losses at line 48 is better than that of line 45.

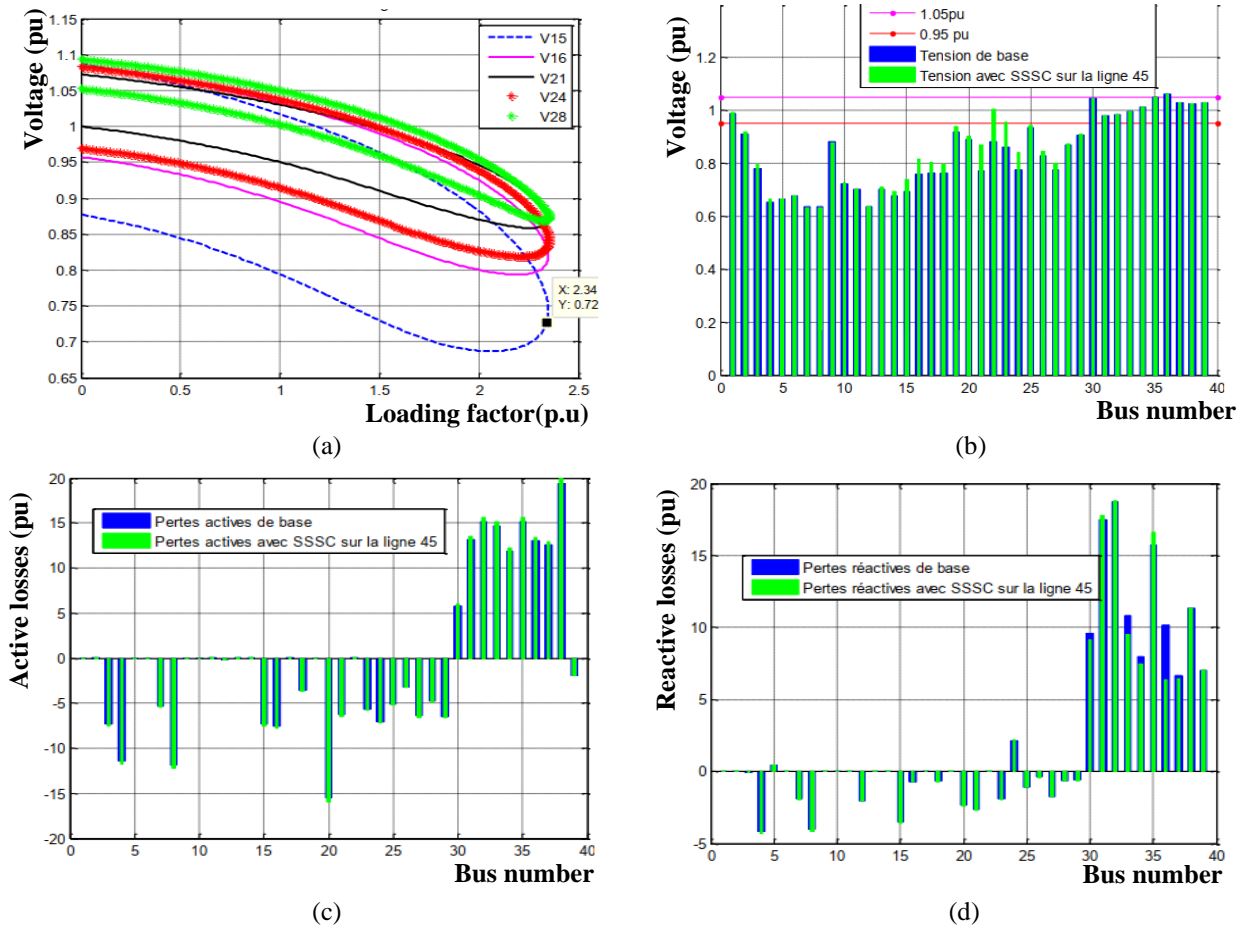


Figure 8: (a) V(P) curve of area 3 with SSSC on line 45, (b) System voltage profiles with SSSC on line 45 and power loss profiles with SSSC on line 45, (c) Active, and (d) Reactive

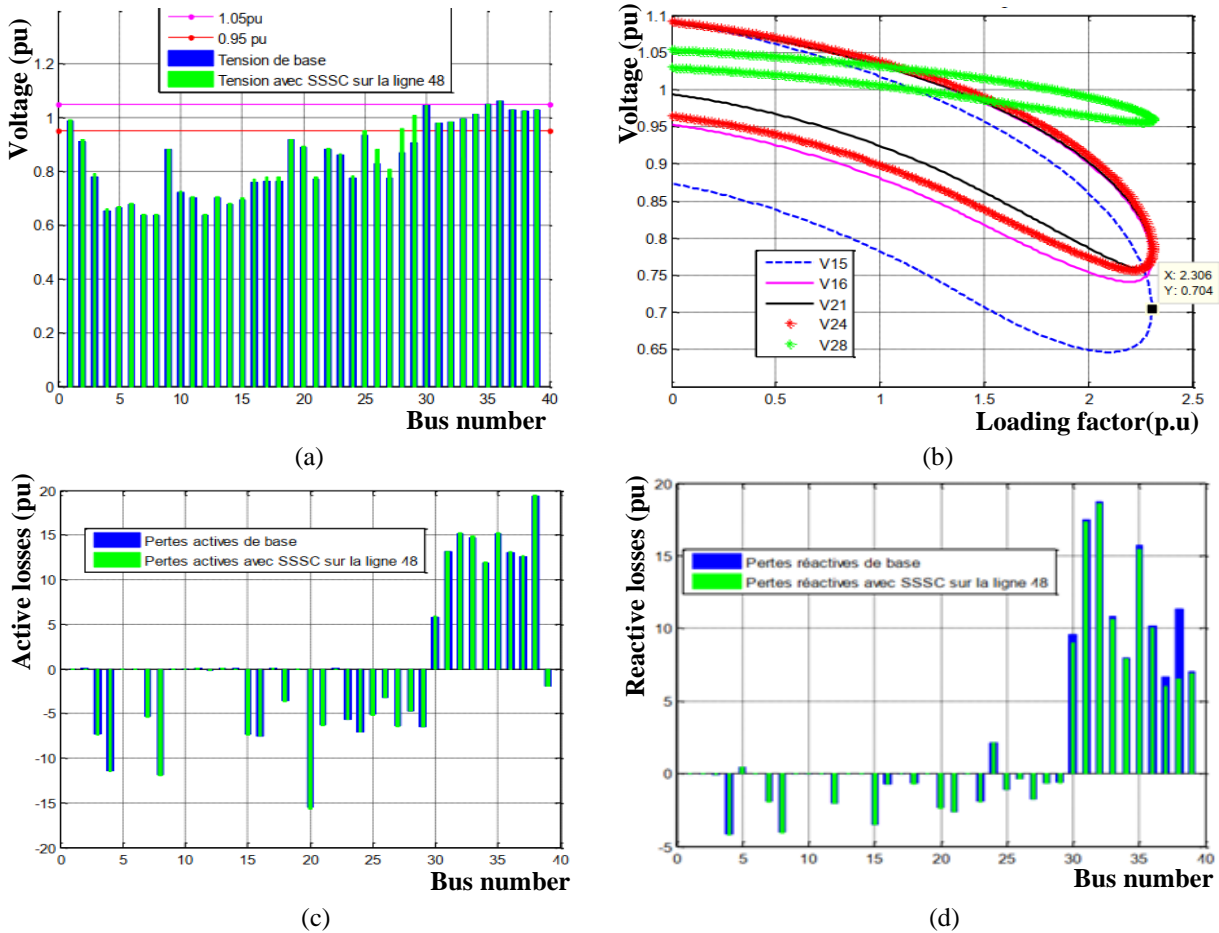


Figure. 9: (a) System voltage profiles with SSSC on line 48, (b) V(P) curve of zone 3 with SSSC on line 48 and power loss profiles with SSSC on line 48, (c) Active, and (d) Reactive

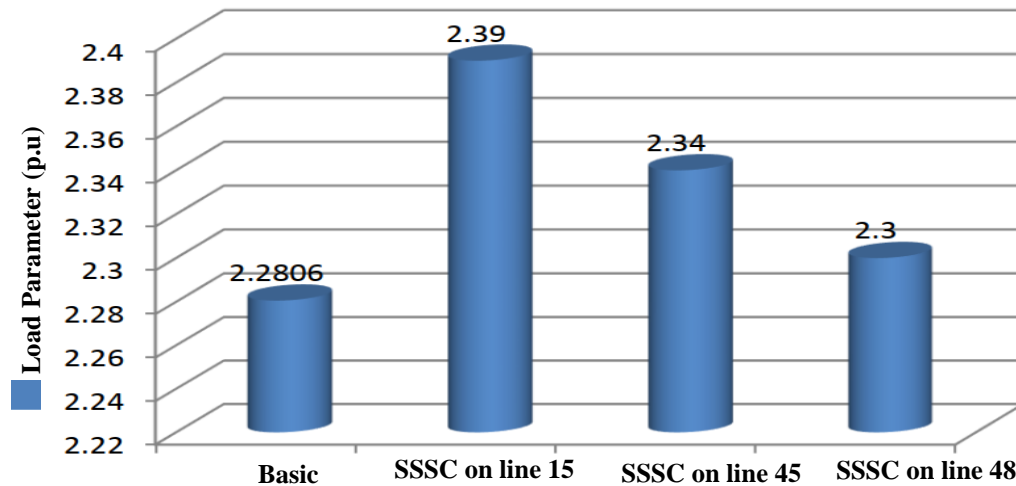


Figure. 10 Maximum load factor with SSSC

#### 4.4 SSSC inserted on line 48

Figs. 9(a), 9(b), 9(c), and 9(d) show the V(P) curves, the voltage profile and the real and reactive loss profile of the test system after the installation of the FACT SSSC devices, respectively. The simulation results show that the voltage profile, after

the addition of the SSSC on line 48, is not better compared to the SSSC inserted on line 45. While the active and reactive loss profile after adding SSSC on line 48 is better than that of SSSC inserted on line 45. Therefore, the reduction rate of real and reactive power losses at line 48 is better than that of line 45.

Figs. 10 and 11 show the load factors ( $\lambda$ ) and the active and reactive losses of lines 15, 45 and 48

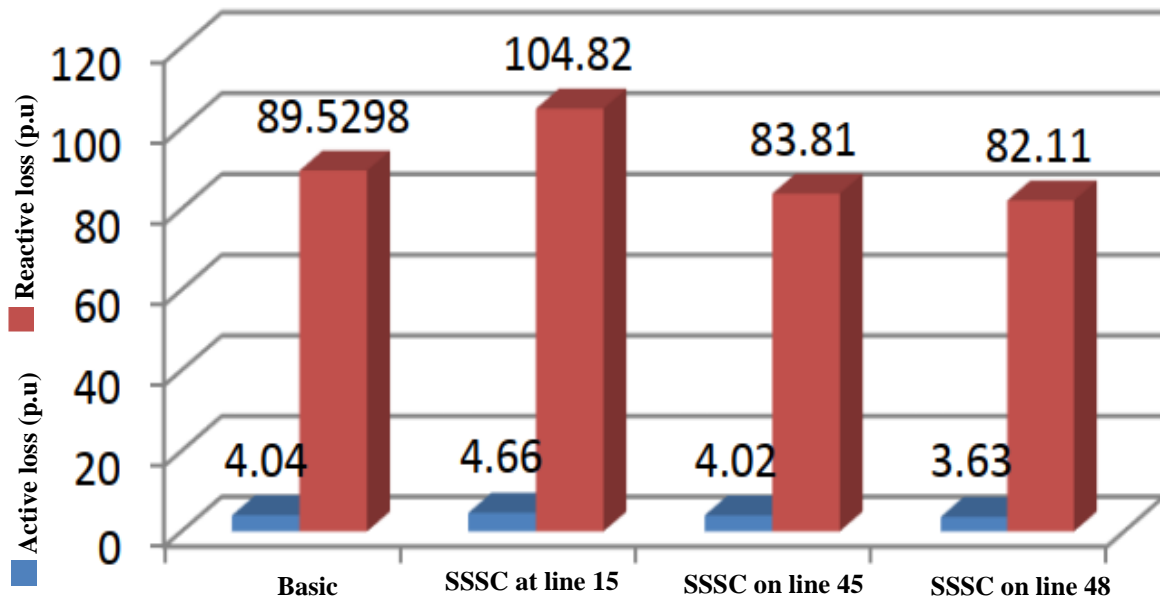


Figure. 11 Total active and reactive losses for the various SSSC locations

without and with the SSSC device, respectively, so that the actual losses are increased by 0.62 p.u on line 15 for a load demand of 2.39 p.u, reduced by 0.02 p.u on line 45 for a load demand of 2.34 p.u and reduced by 0.41 p.u on line 48 for a load demand of 2.3 p.u. While the reactive losses are increased by 15.29 p.u on line 15 for a load demand of 2.39 p.u, reduced by 5.72 p.u on line 45 for a load demand of 2.34 p.u and reduced by 7.42 p.u on line 48 for a load demand of 2.3 p.u. The results show that the reduction rate of real and reactive power losses is better on line 48 than on line 45. La réduction des pertes est compensée par la réduction de la production de l'électricité, ce qui permet d'équilibrer le système électrique.

## 5. Conclusion

This paper proposes a technique based on the CPF method coupled with bifurcation theory for the implementation of SSSC on the New England transmission system suitable line to improve the efficiency of the transmission system, using two indices: the voltage profile and the real and reactive loss profile. The results show that the weakest bus in the IEEE-39 bus power network is bus 8. The 8 bus is served by lines 15, 45 and 48. Based on the proposed method, the optimal location for the SSSC is line 45. The SSSC is capable of improving the voltage profile of the power system, reducing real and reactive power losses and improving local system performance (i.e. in the area where it is implemented). The optimisation results show that the CPF method coupled with bifurcation theory provides valid solutions when implemented for

FACTS devices on power systems. This paper represents the first work that applies the CPF analysis and optimisation technique coupled with bifurcation theory to find the optimal placement of the FACT SSSC device on the IEEE- 39 100 kV bus power network.

## Conflicts of interest

The authors declare no conflict of interest

## Author contributions

Najib Ababssi and El Alami Semma carried out a study on the implementation of the optimal location of the SSSC on the IEEE-39 bus network and the paper structure. Najib Ababssi has developed a mathematical model of the SSSC device and implemented it in analysis and simulation software, called PSAT, to study its impact on voltage collapse. Ababssi Najib and Azeddine Loulijat wrote the paper. Najib Ababssi and Azeddine Loulijat contributed to reviewing the paper. All authors read and approved the final manuscript.

## References

- [1] P. Dorile, D. Jagessar, L. Guardado, S. Jagessar, and R. A. M. Cann, "Power System Stabilization of a Grid Highly Penetrated from a Variable-Speed Wind Based Farm through Robust Means of STATCOM and SSSC", In: *Proc. of 2021 16th Int. Conf. Eng. Mod. Electr. Syst. EMES 2021 - Proc.*, 2021, doi: 10.1109/EMES52337.2021.9484110.

- [2] I. E. Nkan, E. E. Okpo, U. B. Akuru, and O. I. Okoro, "Contingency Analysis for Improved Power System Stability of the Nigerian 330 Kv, 48-Bus System Using Series Facts Controllers", *SSRN Electron. J.*, No. November, 2021, doi: 10.2139/ssrn.3735370.
- [3] O. Sharma, "A Review Article of SSSC based Power Quality Improvement", *Int. J. Res. Appl. Sci. Eng. Technol.*, Vol. 8, No. 7, pp. 1812–1817, 2020, doi: 10.22214/ijraset.2020.30658.
- [4] S. N. Ashida, S. M. Z. N. D. Shahirah, M. Hasmainsi, Z. M. Yasin, and A. N. Fadilah, "Multi-machine transient stability by using static synchronous series compensator", *Int. J. Power Electron. Drive Syst.*, Vol. 11, No. 3, pp. 1249–1258, 2020, doi: 10.11591/ijpeds.v11.i3.pp1249-1258.
- [5] S. Chaine and M. Tripathy, "Performance of static synchronous series compensator and superconducting magnetic energy storage controllers for frequency regulation in two area hybrid wind-thermal power system using Cuckoo Search Algorithm", *Eng. Reports*, Vol. 3, No. 4, pp. 1–13, 2021, doi: 10.1002/eng2.12313.
- [6] D. Kushwaha, and P. Dubey "Application of Static Synchronous Series Compensator for Power Flow Improvement in Electrical Power Transmission System", *International Journal of Modern Engineering & Management Research*, Vol. 8, No. 4, pp. 5–10, 2020.
- [7] S. Sunanda, "Analysis of an Auxiliary Fuzzy Logic Based Static Synchronous Series Compensator", *International Journal for Recent Developments in Science Et Technology*, Vol. 3, No. 2, pp. 44–50, 2019.
- [8] S. N. Waghade and C. Gowder, "Modeling and Simulation of Voltage Source Model of UPFC in an IEEE 9 Bus System for Power Flow Enhancement", *Int. J. Eng. Res.*, Vol. V9, No. 01, pp. 75–80, 2020, doi: 10.17577/ijertv9is010044.
- [9] M. Asad, "The Egyptian International Journal of Improving Power Flow Using Static Synchronous Compensator", *The Egyptian International Journal of Engineering Sciences and Technologym*, Vol. 33, pp. 69–74, 2021.
- [10] P. Sathe, "Effect of Static Synchronous Series Compensator on the behavior of distance relay under fault condition", *Vpenthane.Org*, [Online]. Available: <https://vpenthane.org/web2/assets/files/Ms-PritiSathe-PaperonEffectofSSSConthebehaviorofdistancerelayunderfaultcondition.pdf>.
- [11] S. Galvani, B. M. Ivatloo, M. N. Heris, and S. R. Marjani, "Optimal allocation of static synchronous series compensator (SSSC) in wind-integrated power system considering predictability", *Electr. Power Syst. Res.*, Vol. 191, No. October 2020, p. 106871, 2021, doi: 10.1016/j.epsr.2020.106871.
- [12] A. Udaratin, K. Loginov, A. Nemirovskiy, N. Rozhentsova, and E. Gracheva, "Modelling of emergency modes with FACTS devices installed", *E3S Web Conf.*, Vol. 178, pp. 4–8, 2020, doi: 10.1051/e3sconf/202017801052.
- [13] O. Sharma, "Power System Oscillation Damping and Stability Enhancement using Static Synchronous Series Compensator (SSSC)", *Int. J. Res. Appl. Sci. Eng. Technol.*, Vol. 8, No. 7, pp. 1818–1828, 2020, doi: 10.22214/ijraset.2020.30659.
- [14] L. Vanfretti and F. Milano, "Experience with PSAT (Power System Analysis Toolbox) as free and open-source software for power system education and research", *Int. J. Electr. Eng. Educ.*, Vol. 47, No. 1, pp. 47–62, 2010, doi: 10.7227/ijeee.47.1.5.
- [15] N. Ababssi, E. Semma, and A. Loulijat, "Implementation Optimal Location of STATCOM on the IEEE New England Power System Grid ( 100 kV )", *International Journal of Intelligent Engineering and Systems*, Vol. 15, No. 3, pp. 441–454, 2022, doi: 10.22266/ijies2022.0630.37.
- [16] S. Kumar, A. Kumar, and N. K. Sharma, "Analysis of power flow, continuous power flow and transient stability of IEEE-14 bus integrated wind farm using PSAT", In: *Proc. of Int. Conf. Energy Econ. Environ. - 1st IEEE Uttar Pradesh Sect. Conf. UPCON-ICEEE 2015*, pp. 12–17, 2015, doi: 10.1109/EnergyEconomics.2015.7235099.
- [17] Q. Wang, H. Song, and V. Ajjarapu, "Continuation-Based Quasi-Steady-State Analysis", *IEEE Transactions on Power Systems*, Vol. 21, No. 1, pp. 171–179, 2006.
- [18] J. Zhao, X. Fan, C. Lin, and W. Wei, "Distributed continuation power flow method for integrated transmission and active distribution network", *J. Mod. Power Syst. Clean Energy*, Vol. 3, No. 4, pp. 573–582, 2015, doi: 10.1007/s40565-015-0167-2.
- [19] J. Qi, W. Zhao, and X. Bian, "Comparative Study of SVC and STATCOM Reactive Power Compensation for Prosumer Microgrids with DFIG-Based Wind Farm Integration", *IEEE Access*, Vol. 8, pp. 209878–209885, 2020, doi: 10.1109/ACCESS.2020.3033058.

- [20] M. Z. Laton, I. Musirin, and T. K. A. Rahman, "Voltage stability assessment via continuation power flow method", *Int. J. Electr. Electron. Syst. Res.*, Vol. 1, No. June, pp. 71–78, 2008, [Online]. Available: <http://ieesr.uitm.edu.my/IEESR/Vol.1/vol.1/article8.pdf>.
- [21] K. Bisht, D. Kumar, and K. S. Bedi, "Enhancement of Power Transfer Capacity and Transmission Efficiency using SSSC", *Int. J. Eng. Adv. Technol.*, Vol. 9, No. 3, pp. 2846–2850, 2020, doi: 10.35940/ijeat.c5999.029320.
- [22] S. R. Gaigowal, R. S. Khonde, and D. N. Katole, "SSSC to control Power flow in the Line", *J. Univ. Shanghai Sci. Technol.*, Vol. 23, No. 1, pp. 44–49, 2021, doi: 10.51201/jusst12530.

## Appendix

IEEE	Institute of Electrical and Electronics Engineers
p.u	Relative value system (Per unit)
CPF	Continuation Power Flow
PF	Power Flow
LF	Load Flow
PSAT	Power System Analysis Toolbox
FACTS	Flexible Alternating Current Transmission System
SSSC	Static Synchronous Serie Compensator
V	Vector voltage magnitude
$\lambda$	Load factor
TCSC	Thyristor controlled series compensator
VSC	Voltage Source Converter
$P_{G0}$	Active power of generator
$P_{L0}$	Active load power
$P_s$	Supply bids
$P_D$	Demand bids
$\theta$	Phase Vector
$X_L$	Transmission Line Reactance

## List of symbols

U	Voltage generated by capacitor
I	line current
$X_C$	Capacitive reactance capacitor
X	Total network reactance
$U_L$	Voltage generated by SSSC
$U_q$	Line voltage component on the q-axis
$U_1$	Source voltage
$U_2$	Load voltage
$I_q$	Line current component on the q-axis